

# Studies on the Formation of DNA–Cationic Lipid Composite Films and DNA Hybridization in the Composites

Murali Sastry,<sup>\*,†</sup> Vidya Ramakrishnan,<sup>†</sup> Mrunalini Pattarkine,<sup>‡</sup> and Krishna N. Ganesh<sup>\*,‡</sup>

Materials and Organic Chemistry (Synthesis) Divisions, National Chemical Laboratory, Pune - 411008, India

Received: September 26, 2000; In Final Form: February 6, 2001

The formation of composite films of double-stranded DNA and cationic lipid molecules (octadecylamine, ODA) and the hybridization of complementary single-stranded DNA molecules in such composite films are demonstrated. The immobilization of DNA is accomplished by simple immersion of a thermally evaporated ODA film in the DNA solution at close to physiological pH. The entrapment of the DNA molecules in the cationic lipid film is dominated by attractive electrostatic interaction between the negatively charged phosphate backbone of the DNA molecules and the protonated amine molecules in the thermally evaporated film and has been quantified using quartz crystal microgravimetry (QCM). Fluorescence studies of DNA–ODA composite films obtained by sequential immersion of the ODA matrix in the complementary single-stranded DNA solutions using ethidium bromide intercalator clearly showed that the hybridization of the DNA single strands had occurred within the composite film. Furthermore, fluorescence studies of the preformed double-stranded DNA–ODA biocomposite film indicated DNA entrapment without distortion to the native double-helical structure. The DNA–ODA biocomposite films have been further characterized with Fourier transform infrared (FTIR) and X-ray photoelectron spectroscopy (XPS) measurements. The DNA–fatty lipid composite films would serve as model systems for understanding DNA–membrane interactions as well as in the study of DNA–drug/protein interactions. This approach also shows promise for the synthesis of patterned DNA films and consequent application in disease detection and genome sequencing.

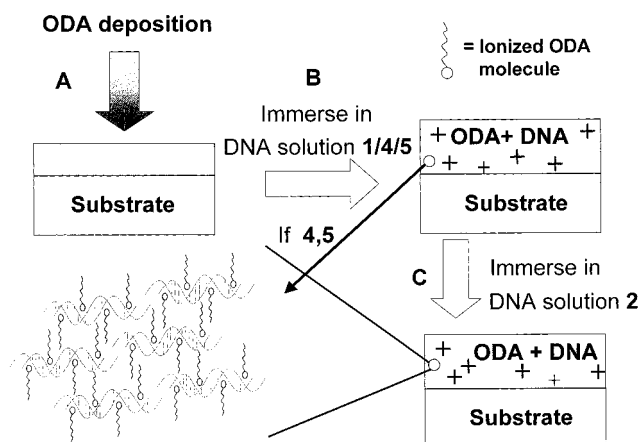
## Introduction

The immobilization of DNA in different matrixes and on planar supports is an exciting area of current research. Entrapment of DNA in cationic liposomes has important application in the development of nonviral DNA vectors in gene therapy.<sup>1–3</sup> Many different routes are being attempted for the immobilization of DNA on planar surfaces, some of the more thoroughly studied methods being assembly at the air–water interface with Langmuir monolayers,<sup>4</sup> self-assembly of thiolated DNA and PNA (peptide nucleic acids) on gold surfaces,<sup>5</sup> and attachment to terminally functionalized self-assembled monolayers (SAMs) via electrostatic<sup>6</sup> and intercalation interactions.<sup>7</sup> The immobilization of single-stranded DNA on planar surfaces to yield DNA chips, in particular, is the focus of intense research due to potential applications in disease diagnosis and genome sequencing.<sup>5</sup>

Developing on our earlier work on the electrostatic entrapment of charged nanoparticles<sup>8</sup> and protein molecules<sup>9</sup> in fatty lipid matrices, we demonstrate herein the immobilization of synthetic (both single-stranded and preformed helical structures) and calf-thymus DNA in thermally evaporated films of cationic fatty amine molecules by a simple beaker-based immersion technique. The procedure is illustrated in Scheme 1 and will be discussed subsequently. The entrapment of DNA molecules from solution in the lipid matrix is driven by electrostatic interaction between the negatively charged DNA and cationic octadecyl-

## SCHEME 1 : Diagram Showing the Various Stages of the DNA–ODA Composite Film Formation<sup>a</sup>

Schematic 1 Sastry *et al*



<sup>a</sup> Step A: deposition of ODA on solid substrates by thermal evaporation. Step B: complexation of single-stranded DNA 1/double-stranded calf-thymus DNA 4/double-stranded DNA 5 with ODA molecules in the film during immersion in the different DNA solutions. Step C: sequential immersion in single-stranded DNA 2 solution after entrapping the complementary strands 1. In step C, a negative experiment may also be carried out by immersion of the 1–ODA composite film in the noncomplementary oligonucleotide solution, 3. The magnified section shows the possible microscopic structure of the DNA–ODA complexes.

amine (ODA) molecules. In the case of double-helical DNA structures, the extraction from solution and formation of DNA–lipid composite films occurs without distortion to their double-helical structure. A particularly exciting result of our investi-

\* Corresponding authors. Tel.: +91 20 5893044 (M.S.), +91 20 5893153 (K.N.G.). Fax: +91 20 5893044(M.S), +91 20 5893153 (K.N.G.). E-mail: sastry@ems.ncl.res.in (M. S.), kng@ems.ncl.res.in (K. N. G.)

<sup>†</sup> Materials Division, National Chemical Laboratory.

<sup>‡</sup> Organic Chemistry (Synthesis) Division, National Chemical Laboratory.

gation is the demonstration that sequential immersion of the fatty amine film in solutions of complementary single-stranded oligonucleotide sequences leads to the hybridization of the DNA single strands within the composite film to yield double-helical structures. We would like to point out that the single-stranded DNA solutions are prepared in deionized water and, therefore, under conditions where hybridization does not occur spontaneously in the bulk of the solution. The cationic lipid molecules thus appear to play a double role, that of electrostatic extraction/immobilization as well as that of counterions screening the repulsive electrostatic interactions between the single-stranded DNA molecules, thereby facilitating the hybridization. The formation of the lipid–DNA composite films and the hybridization of complementary oligonucleotides within the composite material have been followed by quartz crystal microgravimetry (QCM), fluorescence spectroscopy and Fourier transform infrared spectroscopy (FTIR) measurements, while a chemical characterization of the films has been carried out by X-ray photoemission spectroscopy (XPS). Presented below are details of the investigation.

### Experimental Details

Oligonucleotides of the sequences GGAAAACTTCGTGC (1), GCACGAAGTTTTTCC (2), and AGAAGAAGAAA-GAA (3) were synthesized by  $\beta$ -cyanoethyl phosphoramidite chemistry on a Pharmacia GA plus DNA synthesizer and purified by FPLC and rechecked by RP HPLC. The oligonucleotides 1 and 2 are complementary, while 1 and 3 are noncomplementary. 250 and 425 Å thick ODA films (Aldrich) were thermally evaporated onto gold-coated 6 MHz AT-cut quartz crystals, quartz substrates, and Si (111) wafers for QCM, contact angle measurements, fluorescence spectroscopy, Fourier transform infrared (FTIR), and X-ray photoelectron spectroscopy (XPS) measurements (Schematic 1, step A). The films were deposited in an Edwards E306A vacuum coating unit operating at a pressure of better than  $1 \times 10^{-7}$  Torr. The thickness of the deposited films was monitored in-situ using an Edwards QCM. The thickness of the films was cross-checked using ellipsometry.

The incorporation of the DNA molecules into the fatty amine films and the hybridization of the single-stranded DNA molecules 1 and 2 were studied as per the protocol illustrated in Schematic 1. Step B of the procedure consists of immersion of 250 Å thick ODA films on QCM crystals/quartz substrates/Si (111) wafers in  $10^{-6}$  M aqueous, deionized DNA solutions (pH 6.8) of 1 and calf-thymus DNA [CT-DNA (1000 bp), 4]. The entrapment of the DNA molecules into the fatty lipid matrix was followed by measuring the frequency changes in time of the ODA-coated QCM crystal. This was achieved by ex-situ measurement of the QCM resonant frequency after thorough washing and drying of the crystals using an Edwards FTM5 frequency counter. This frequency counter had a resolution and stability of 1 Hz. The frequency change ( $\Delta f$ ) was converted to mass loading ( $\Delta m$ ) using the relationship  $\Delta m = 12.1 \Delta f$  (ng/cm<sup>2</sup>). Preformed DNA duplexes (5) obtained by mixing equimolar quantities of 1 and 2 under standard hybridization conditions<sup>10</sup> were also incorporated in the ODA films by similar immersion in the double-stranded DNA solution ( $10^{-6}$  M concentration) and the QCM mass uptake kinetics studied. To study the role of the film thickness on the DNA entrapment process, we also studied the mass uptake in a 425 Å thick ODA film on a QCM crystal during immersion in the preformed DNA duplex solution 5 ( $10^{-6}$  M concentration). As will be seen subsequently, this important experiment enables one to ascertain whether the DNA molecules are entrapped within the lipid matrix or simply immobilized on the fatty amine film surface.

After the optimum immersion times were determined from the QCM measurements mentioned above, 250 Å thick ODA films on Si (111) wafers were immersed in  $10^{-6}$  M solutions of 4 and 5, thoroughly washed, and dried for FTIR measurements. The FTIR measurements were carried out in the diffuse reflectance mode on a Shimadzu PC-8201 PC instrument at a resolution of 4 cm<sup>-1</sup>. A sufficient number of scans (at least 256) was taken to obtain a good signal-to-noise ratio. Contact angle measurements of 250 Å thick ODA films on Si substrates before and after immersion in 5 as well as after sequential immersion in oligonucleotide solutions 1 and 2 were carried out by the sessile water drop method (1  $\mu$ L water droplet) using a Rame-Hart 100 goniometer. The 250 Å thick ODA–5 composite film on Si (111) substrate was further studied by XPS. XPS measurements of the C 1s, N 1s, and P 2p core levels was carried out on a VG Microtech ESCA 3000 instrument at a base pressure better than  $1 \times 10^{-9}$  Torr with unmonochromatized Mg K $\alpha$  radiation (1253.6 eV energy). The measurements were made in the constant analyzer energy (CAE) mode at a pass energy of 50 eV. This leads to an overall resolution of  $\sim 1$  eV in the measurements. The chemically distinct components in the core level spectra were resolved by a nonlinear least-squares fitting algorithm after background removal by the Shirley method.<sup>11</sup> The alignment of the different core levels was done taking the binding energy of adventitious carbon to be 285 eV.

The formation of double-helical structures by hybridization of the complementary oligonucleotide sequences 1 and 2 within the DNA–ODA composite film may be conveniently studied by introduction of the well-known fluorescent intercalator, ethidium bromide. Enhanced fluorescence from the ethidium bromide molecules occurs on intercalation in the double-helical DNA structures<sup>12</sup> and may be used to follow the hybridization process. ODA films 250 Å thick on quartz substrates were immersed for 4 h in aqueous solutions of the following: (1) 1.26  $\mu$ M ethidium bromide intercalator, (2) 1 ( $10^{-6}$  M concentration) with 1.26  $\mu$ M of intercalator (Schematic 1, step B), (3) 1 followed by immersion in the complementary DNA 2 ( $10^{-6}$  M concentration) with intercalator (Schematic 1, step C), and (4) 5 ( $10^{-6}$  M concentration) with the intercalator (Schematic 1, step B) and 5) in 1, followed by immersion in noncomplementary DNA 3 with the intercalator. The fluorescence measurements of the ODA–DNA composite films were carried out on a Perkin-Elmer model LS 50-B spectrofluorimeter at 25 °C, with slit widths of 5 nm for excitation at 460 nm and 10 nm for the emission monochromators. The excitation wavelength was chosen to match the resonance from the ethidium bromide intercalator. The films grown on quartz substrates were cut to fit precisely in the quartz cuvette normally used for liquid samples. It is to be noted that in the above fluorescence measurements, films 1, 2, and 5 are controls.

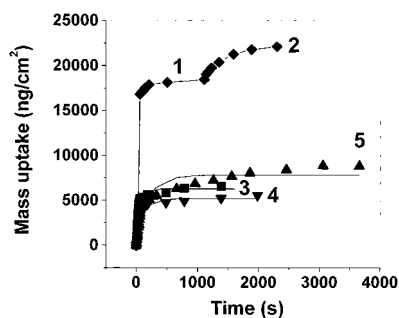
### Results and Discussion

Figure 1 depicts the QCM mass uptake kinetics during immersion of 250 Å thick ODA films in aqueous solutions of the DNA molecules 1, 5, and 4 (curves 1, 3, and 4 respectively). The figure also shows the sequential mass uptake recorded from the ODA film first complexed with single-stranded DNA 1 (curve 1, Figure 1; step B, Schematic 1) during immersion in the complementary single-stranded DNA 2 (curve 2, diamonds; step C, Schematic 1) as well as the mass uptake recorded during entrapment of DNA 5 in a 425 Å thick ODA film (curve 5). It is observed that the mass uptake is highest for the single-stranded DNA 1. Furthermore, the mass uptake of the complementary DNA strand 2 into the ODA–1 composite film is ca. 20% of the mass uptake recorded during diffusion of DNA 1

**TABLE 1: DNA-to-ODA Charge Ratios in the Different DNA–ODA Composite Films Estimated from an Analysis of the QCM Mass Uptake Data Shown in Figure 1**

diffusion experiment	ODA matrix mass (ng/cm <sup>2</sup> )	DNA equilibrium mass loading (ng/cm <sup>2</sup> )	single-stranded DNA/duplex DNA mol wt <sup>a</sup>	DNA/ODA charge ratio
single-stranded DNA <b>1</b>	2420 <sup>b</sup>	21920	5280	7.2
double-stranded DNA <b>5</b>	2420 <sup>b</sup>	6290	10560	2.1
double-stranded DNA <b>5</b>	4115 <sup>c</sup>	8760	10560	1.75
double-stranded calf-thymus DNA <b>4</b>	2420 <sup>b</sup>	5190	660000	1.8

<sup>a</sup> The DNA molecular weights are calculated using the formula  $330 \times \text{number of bases in sequence} \times 1 \text{ or } 2$  (depending on whether the DNA is single-stranded or duplex). <sup>b</sup> These data corresponds to the 250 Å thick ODA film. <sup>c</sup> These data correspond to the 425 Å thick ODA film.



**Figure 1.** QCM mass uptake as a function of time of immersion of a 250 Å thick ODA film in 1  $\mu\text{M}$  solutions of **1** (curve 1, diamonds), the single-stranded DNA **1**–ODA film shown as curve 1 during immersion in **2** (curve 2, diamonds), **5** (curve 3, squares), and **4** (curve 4, down triangles). The figure also shows the QCM mass uptake recorded during immersion of a 425 Å thick ODA film in 1  $\mu\text{M}$  solution of **5** (curve 5, up triangles).

in the first immersion cycle. This indicates blockage of the diffusion pathways into the ODA–**1** composite film available to DNA **2** and, therefore, incomplete hybridization of the DNA molecules into double-helical structures (see fluorescence measurements below). The number of DNA molecules entrapped within the lipid matrix and thereby the charge ratio of the DNA molecules to the ionized ODA molecules in the lipid matrix may be easily estimated by simple back-of-the-envelope calculations.<sup>13</sup> The equilibrium DNA mass loadings and the DNA/ODA charge ratios are listed in Table 1, along with the relevant parameters used in the calculations for the QCM data shown in Figure 1. It is interesting to note from Table 1 that in all cases, there is overcompensation of the positive charge on the ODA molecules in the composite film by the negative charge of the DNA molecules. While the degree of overcompensation is largest in the case of the single-stranded DNA–ODA composite films, the DNA/ODA charge ratio settles at close to 2 for both the synthetic (DNA **5**) and natural DNA duplex structures (calf-thymus DNA **4**). Such a charge overcompensation is known to occur during complexation of large inorganic ions such as Keggin anions at the air–water interface<sup>14</sup> as well as in electrostatically formed multilayers of cationic and anionic polyelectrolyte films, in multilayer films of polyelectrolytes and DNA,<sup>15</sup> and in multilayers of positively and negatively charged nanoparticles.<sup>16</sup> This important result indicates that the DNA molecules can be complexed with lipid molecules at concentrations higher than that previously reported<sup>17</sup> and may serve as model systems for understanding densely packed DNA in supramolecular organizes such as chromatin.<sup>18</sup> At this stage, we are unable to comment on why the degree of overcompensation is much larger in the case of the single-stranded DNA molecules **1** and **2** vis-à-vis the double-stranded DNA molecules **4** and **5**.

There is clearly substantial entrapment of the DNA molecules in the ODA film in all the DNA molecules studied herein. There

are two possible modes by which the DNA molecules may be immobilized in the ODA films, viz., purely surface binding versus formation of a DNA–ODA complex film as shown in the magnified section of Schematic 1. To resolve this issue, we performed contact angle measurements on a 250 Å thick ODA film on a quartz substrate before and after immersion of the film in  $10^{-6}$  M concentrated double-stranded DNA **5** solution for 4 h and obtained the values of  $90^\circ$  and  $89^\circ$ , respectively. Similar contact angle measurements of a 250 Å thick ODA film before and after sequential immersion in  $10^{-6}$  M DNA solutions **1** and **2** for 4 h yielded values of  $92^\circ$  and  $90^\circ$ , respectively. These values represent averages over 10 measurements carried out over the whole film surface and indicate a hydrophobic surface in both the bare and DNA-loaded films. Thus, the DNA molecules complex with the ODA molecules by electrostatic interactions to yield a composite material such as that shown in Schematic 1 (magnified section). The contact angle results of the latter experiment, wherein the complementary oligonucleotides were entrapped sequentially in the ODA film, clearly show that hybridization of the DNA molecules (as will be established below) occurs within the DNA–ODA composite film and not on the film surface. A simple calculation serves to add further weight to this conclusion. The equilibrium mass loading for the DNA **5**–ODA composite film (250 Å thickness) is  $6290 \text{ ng/cm}^2$  (Table 1). Assuming purely surface binding of the DNA molecules, this works out to ca.  $3.6 \times 10^{14}$  molecules/cm<sup>2</sup>. The overall projected area of this density of DNA molecules is thus  $55 \text{ Å}$  (length of 16-mer DNA molecule)  $\times$   $20 \text{ Å}$  (diameter of double helix)  $\times$   $3.6 \times 10^{14} \sim 40 \text{ cm}^2$ . In other words, the mass loading of DNA measured would lead to nearly 40 monolayers of DNA molecules in a close-packed state on the surface of the ODA film. This should lead to a significant reduction in the contact angle, which is not the case.

Figure 2 shows the fluorescence emission spectra recorded from 250 Å thick ODA films on quartz after immersion for 4 h in aqueous solutions of ethidium bromide intercalator (curve 1), single-stranded DNA **1** with  $1.26 \mu\text{M}$  of intercalator (curve 2), single-stranded DNA **1** followed by immersion in the noncomplementary single-stranded DNA **3** with intercalator (curve 3), double-stranded DNA **4** with the intercalator (curve 4), and single-stranded DNA **1** followed by immersion in complementary single-stranded DNA **2** with the intercalator (curve 5). Figure 2 also shows the emission spectrum from the sequentially formed DNA–ODA composite film (as in curve 5) after heating at  $40^\circ \text{C}$  for 20 min (curve 6). It is seen that there is no emission from the intercalator in the bare ODA film (curve 1) as well as from composite films of single-stranded DNA **1** (curve 2) and single-stranded DNA **1** complexed with noncomplementary DNA single strands **3** (curve 3), even after heating. A strong emission signal is clearly seen for the double-stranded DNA **5**–ODA composite film (curve 4). This result clearly indicates that the DNA molecules in the DNA–ODA composite material are entrapped without distortion to the

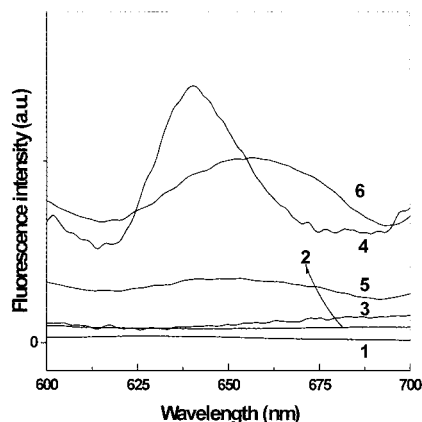


**Figure 2.** Fluorescence emission spectra for 250 Å thick ODA films on quartz after immersion in the following solutions for 4 h in aqueous solutions of ethidium bromide (curve 1), a mixture of the single-stranded DNA **1** and intercalator (curve 2), single-stranded DNA **1** followed by noncomplementary single-stranded DNA **3** and intercalator (curve 3), hybridized DNA **5** and intercalator (curve 4), single-stranded DNA **1** followed by complementary single-stranded DNA **2** and intercalator (curve 5), and the film shown as curve 5 after heating at 40 °C for 20 min (curve 6).

double-helical structure, thereby permitting the binding of ethidium bromide.<sup>12</sup> The fluorescence emission spectrum which was weak for the film formed by sequential immersion in solutions of complementary oligonucleotides **1** and **2** (curve 5) increased significantly after heating (curve 6). This is due to the formation of duplex structures after heating, aided by the thermal diffusion of DNAs **1** and **2**. Thus, hybridization of the DNA strands is possible within the DNA-ODA composite film. The observed increase in the fluorescence intensity after heating is not due to the entrapment of the fluoroprobe alone in the hydrophobic matrix, since such an effect was not seen in samples without DNA (Figure 2, curve 1) or composed of noncomplementary DNA strands (Figure 2, curve 3). This strongly supports the conclusion that hybridization of DNA **1** and its complementary DNA **2** in the ODA biocomposite film is indeed responsible for the enhanced fluorescence signal. We would like to point out at this stage that the hybridization of DNA **1** and **2** occurs only within the composite film since the entrapment is accomplished under DNA solution conditions (deionized water) where hybridization does not occur spontaneously in solution.<sup>10</sup> Thus, the ODA molecules in the composite film act like counterions to screen the repulsive electrostatic interactions between the negatively charged DNA single-strands enabling hybridization to occur. Interestingly, it is observed that while the emission maximum occurs at ca. 640 nm for the double-stranded DNA film (curve 4), it was shifted to ca. 660 nm and accompanied by broadening for the in-situ hybridized DNA-ODA film (curve 6). This may be due to differences in the polarity of the environment experienced by the fluorescent probe due to different binding modes with the DNA duplexes in the two situations. While the features of curve 4 are typical of intercalation, the broad, red-shifted fluorescence (curve 6) is indicative of binding at a second site, such as that on the DNA duplex surface by mere electrostatic interaction. This interpretation, which is also consistent with the literature observation on DNA-ethidium bromide complexes,<sup>12</sup> is a definite consequence of DNA duplex formation within the composite film.

FTIR spectra recorded from 250 Å thick ODA films on Si (111) substrates before and after immersion in  $10^{-6}$  M solutions of double-stranded DNA **5** and calf-thymus DNA **4** are shown as curves a, b, and c respectively in Figure 3. Three strong resonances at  $1230\text{ cm}^{-1}$ ,  $1065\text{ cm}^{-1}$ , and  $964\text{ cm}^{-1}$  (features

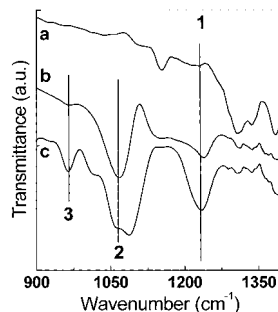


**Figure 3.** FTIR spectra of 250 Å thick ODA films on Si (111) substrates before (curve a) and after immersion for 4 h in double-stranded DNA **5** and calf-thymus DNA **4** (curve c) solutions. Three features 1–3 at  $1230$ ,  $1065$ , and  $964\text{ cm}^{-1}$  are labeled in the figure (see text for details).

1–3 in Figure 3) are clearly observed from the DNA-ODA composite films (spectra b and c, Figure 3), which are missing in the as-deposited ODA film (curve a, Figure 3). The  $1230$  and  $964\text{ cm}^{-1}$  bands are due to the backbone  $\text{PO}_2$  antisymmetric stretching and deoxyribose C–C stretching vibrations, respectively, and agree well with literature values of hybridized DNA molecules.<sup>19</sup> The feature at  $1065\text{ cm}^{-1}$  is assigned to the deoxyribose band as well, the presence of which is indicative of Z-DNA double-helical conformation.<sup>20</sup> Such a conformation is known to occur for double-helical DNA molecules in an environment of high ionic strength, as would be the case during complexation with ODA molecules. This result also supports the large red shift observed in the fluorescence emission signal observed from the double-helical DNA-ODA composite films which is a consequence of a highly polar environment (Figure 2, spectra 4 and 6).

The XPS C 1s, P 2p, and N 1s core levels were recorded from a 250 Å thick double-stranded DNA **5**-ODA composite film grown on Si (111) substrate, and the spectra obtained are shown in panels A–C, respectively, of Figure 4. The C 1s spectrum could be decomposed into two components at 285 and 287.5 eV binding energy (curves 1 and 2 respectively, Figure 4A). The low binding energy (BE) component is assigned to electron emission from the hydrocarbon chains of ODA, the sugars and bases in the DNA, while the higher BE component is from the carbons coordinated to the phosphates in the backbone. The P 2p core level, which clearly arises due to electron emission from the phosphate backbone of the entrapped DNA molecules, could be decomposed into a single spin-orbit pair, as shown in Figure 4B. The P  $2p_{3/2}$  BE was evaluated to be 132.8 eV (Figure 4B) and agrees fairly well with reported values of DNA immobilized on self-assembled monolayer surfaces,<sup>21</sup> and it indicates no degradation of the DNA molecules due to electrostatic complexation with the ODA molecules. The N 1s core level showed a single component centered at 399.7 eV (Figure 4C) and is due to the electron emission from the nitrogens in the ODA and base molecules of DNA.

Additional evidence of the retention of the double-helical structure of the DNA molecules within the DNA-OA composite material was provided by UV melting measurements carried out on a 250 Å thick double-stranded DNA **5**-ODA film on quartz.<sup>22</sup> The UV melting curve of this film is shown as Figure 1 of the Supporting Information. A melting transition temperature ( $T_M$ ) of 58 °C was measured for this film clearly showing the double-helical structure of the DNA molecules in the film. Furthermore, the  $T_M$  value is considerably higher than the solution melting temperature value of 41 °C reported for the 16-mer duplexes used in this study.<sup>17</sup> This large shift in the  $T_M$

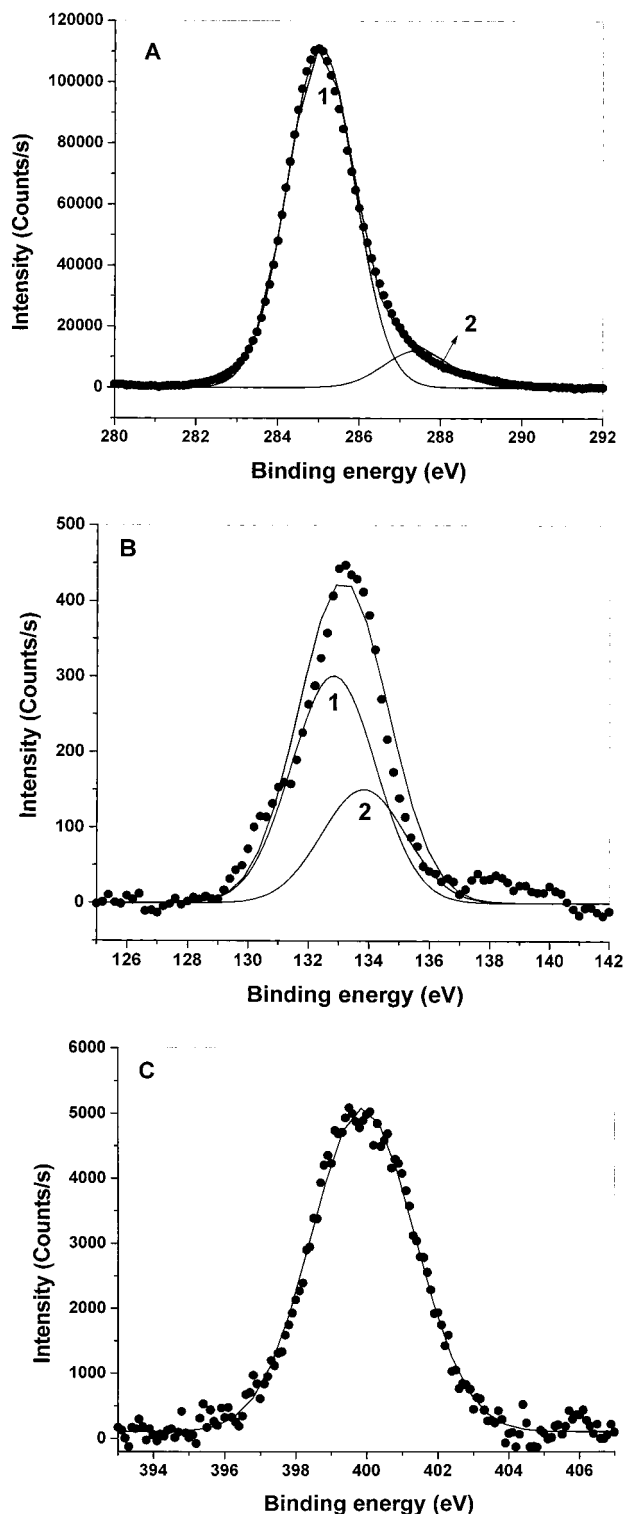


**Figure 4.** (A) C 1s core level spectrum recorded from a 250 Å thick 5-ODA composite film on Si (111) substrate. Two chemically distinct components are shown (see text for details). (B) P 2p core level spectrum from a 250 Å thick 5-ODA composite film on Si (111) substrate. The two 2p spin-orbit components are shown. (C) N 1s core level spectrum from a 250 Å thick 5-ODA composite film on Si (111) substrate. The data are fit to a single Gaussian (see text for details).

value toward higher temperatures indicates considerable stabilization of the double-helical structure by the lipid matrix.

In conclusion, it has been demonstrated that DNA molecules may be electrostatically entrapped in thermally evaporated cationic lipid films by a simple solution immersion procedure without altering the double-helical structure of DNA. Further-

more, sequential immersion of the lipid film in complementary single-stranded DNA solutions leads to hybridization of the DNA molecules within the DNA–cationic lipid composite film and the possible structure illustrated in Schematic 1. Such DNA–lipid composites are expected to be ideal model systems for studying the permeability of DNA and PNA in cell membranes, important for DNA antisense therapeutics.<sup>23</sup> Another exciting possibility is the potential formation of patterned, multi-DNA arrays in DNA chip applications.<sup>5</sup>

**Acknowledgment.** The authors thank Dr. A. B. Mandale, Special Instruments Laboratory, NCL Pune, for assistance with the XPS measurements.

**Supporting Information Available:** One page (Figure 1) of the UV melting curve recorded from a 250 Å thick double-stranded DNA 5-ODA biocomposite film. This material is available free of charge via the Internet at <http://pubs.acs.org>.

## References and Notes

- (1) Radler, J. O.; Koltover, I.; Salditt, T.; Safinya, C. R. *Science* **1997**, *275*, 810.
- (2) Radler, J. O.; Koltover, I.; Jamieson, A.; Salditt, T.; Safinya, C. R. *Langmuir* **1998**, *14*, 4272.
- (3) Lasic, D. D.; Strey, H.; Stuart, M. C. A.; Podgornik, R.; Frederik, P. M. *J. Am. Chem. Soc.* **1997**, *119*, 832.
- (4) (a) Okahata, O.; Kobayashi, T.; Tanaka, K. *Langmuir* **1996**, *12*, 1326. (b) Ijio, K.; Shimomura, M.; Tanaka, M.; Nakamura, H.; Hasebe, K. *Thin Solid Films* **1996**, *284–285*, 780. (c) Shimomura, M.; Nakamura, F.; Ijio, K.; Taketsuna, H.; Tanaka, M.; Nakamura, H.; Hasebe, K. *J. Am. Chem. Soc.* **1997**, *119*, 2341. (d) Kago, K.; Matsuoka, H.; Yoshitome, R.; Yamaoka, H.; Ijio, K.; Shimomura, M. *Langmuir* **1999**, *15*, 5193. (e) Ebara, Y.; Mizutani, K.; Okahata, Y. *Langmuir* **2000**, *16*, 2416. (f) Sastry, M.; Ramakrishnan, V.; Pattarkine, M.; Gole, A.; Ganesh, K. N. *Langmuir* **2000**, *16*, 9142.
- (5) (a) Steel, A. B.; Herne, T. M.; Tarlov, M. *J. Anal. Chem.* **1998**, *70*, 4670. (b) Wang, J.; Nielsen, P. E.; Jiang, M.; Cai, X.; Fernandez, J. R.; Grant, D. H.; Ozsoz, M.; Begleiter, A.; Mowat, M. *Anal. Chem.* **1997**, *69*, 5200.
- (6) Higashi, N.; Inoue, T.; Niwa, M. *J. Chem. Soc., Chem. Commun.* **1997**, 1507.
- (7) Higashi, N.; Takahashi, M.; Niwa, M. *Langmuir* **1999**, *15*, 111.
- (8) (a) Sastry, M.; Patil, V.; Sainkar, S. R. *J. Phys. Chem. B* **1998**, *102*, 1404. (b) Patil, V.; Malvankar, R. B.; Sastry, M. *Langmuir* **1999**, *15*, 8197. (c) Sastry, M. *Curr. Sci.* **2000**, *78*, 1089.
- (9) (a) Gole, A.; Dash, C. V.; Rao, M.; Sastry, M. *J. Chem. Soc., Chem. Commun.* **2000**, 297. (b) Gole, A.; Dash, C. V.; Mandale, A. B.; Rao, M.; Sastry, M. *Anal. Chem.* **2000**, *72*, 1401.
- (10) Cantor, C. R.; Schimmel, P. R. *Biophysical Chemistry, Part III*; W. H. Freeman: New York, 1980.
- (11) Shirley, D. A. *Phys. Rev. B* **1972**, *5*, 4709. An application written by one of us (MS) in Mathcad (a commercial mathematical software package), SHIRL. MCD was used for the analysis. This application is available from the Mathsoft public domain site.
- (12) LePecq, J. B.; Paoletti, C. *J. Mol. Biol.* **1967**, *27*, 87.
- (13) The equilibrium mass uptake after entrapment of DNA 1 followed by 2 in the fatty lipid film is 21 920 ng/cm<sup>2</sup>. The number of DNA molecules corresponding to this mass is:  $(21920 \times 10^{-9} \times 6.024 \times 10^{23})/5280 \approx 2.5 \times 10^{15} \text{ cm}^{-2}$ . The number of ODA molecules corresponding to a deposition of 2420 ng/cm<sup>2</sup> can be similarly shown to be  $5.41 \times 10^{15} \text{ cm}^{-2}$  (the molecular weight of ODA = 269.5). Assuming complete ionization of all the ODA molecules in the lipid matrix, the DNA/ODA charge ratio is  $(2.5 \times 10^{15} \times 16)/5.41 \times 10^{15} \approx 7.4$ . The multiplication by 16 in the numerator is to account for the charges in the 16-mer oligonucleotides used in this study.
- (14) Cuvillier, N.; Rondelez, F. *Thin Solid Films* **1998**, *327–329*, 19.
- (15) Decher, D. *Science* **1997**, *277*, 1232 and references therein.
- (16) (a) Lvov, Y.; Ariga, K.; Onda, M.; Ichinose, I.; Kunitake, T. *Langmuir* **1997**, *13*, 6195. (b) Kumar, A.; Mandale, A. B.; Sastry, M. *Langmuir* **2000**, *16*, 6921.
- (17) Pattarkine, M. V.; Ganesh, K. N. *Biochem. Biophys. Res. Commun.* **1999**, *263*, 41. A maximum DNA:surfactant charge ratio of 0.8 was observed in DNA–cationic lipid micelles in this study.
- (18) (a) Klug, A.; *Philos. Trans. R. Soc. London Ser. A* **1994**, *348*, 167. (b) Trubetskoy, V. S.; Loomis, A.; Slattum, P. M.; Hagstron, J. E.; Budker, V. G.; Wolff, J. A. *Bioconjugate Chem.* **1999**, *10*, 624.

(19) Neault, J. F.; Tajmir-Riahi, H. A. *J. Phys. Chem. B* **1998**, *102*, 1610.

(20) Taillandier, E.; Liquier, J. *Methods Enzymol.* **1992**, *211*, 307.

(21) The BE of 136 eV quoted for the P 2p core level recorded from DNA molecules immobilized on self-assembled monolayer surfaces (see ref 7 above) is, we believe, for the centroid of the core level. The agreement between this BE value and that observed by us would improve if the P 2p envelope of Higashi et al. were decomposed into the 2 p<sub>3/2</sub> and 2 p<sub>1/2</sub> core levels, as done by us.

(22) The UV melting experiments were carried out on Perkin-Elmer Lambda 15 UV/VIS spectrophotometer fitted with a Julabo water circulator with programmed heating accessory. The quartz substrates bearing the films were cut to fit into the cuvette normally used for liquid samples. The DNA–ODA films were heated at a rate of 0.5 °C per min, and the thermal denaturation of the duplex was followed by monitoring changes in the absorbance at 260 nm as a function of temperature.

(23) In *Methods in Enzymology*; Phillips, M. I., Ed.; Academic: San Diego, 2000; Vol. 313.